

# TEMPERATURE DEPENDENCE OF CATHODOLUMINESCENCE FROM $\text{In}_x\text{Ga}_{1-x}\text{As}/\text{GaAs}$ MULTIPLE QUANTUM WELLS

K. RAMMOHAN,\* D.H. RICH,\* AND A. LARSSON\*\*

\*Department of Materials Science and Engineering, University of Southern California, Los Angeles, CA 90089-0241

\*\*Department of Optoelectronics and Electrical Measurements, Chalmers University of Technology, Göteborg, Sweden.

## ABSTRACT

The temperature dependence of the cathodoluminescence (CL) originating from  $\text{In}_{0.21}\text{Ga}_{0.79}\text{As}/\text{GaAs}$  multiple quantum wells has been studied between 86 and 250 K. The CL intensity exhibits an Arrhenius-type dependence on temperature (T), characterized by two different activation energies. The spatial variations in activation energy caused by the presence of interfacial misfit dislocations is examined. The CL intensity dependence on temperature for  $T \lesssim 150$  K is controlled by thermally activated nonradiative recombination. For  $T \gtrsim 150$  K the decrease in CL intensity is largely influenced by thermal re-emission of carriers out of the quantum wells.

## INTRODUCTION

Modern electronic and photonic devices based on heterostructures, such as high-electron mobility transistors (HEMTs)<sup>1</sup> often consist of lattice-mismatched layers exhibiting high crystalline perfection which is thought to be crucial for optimum device performance. The use of lattice-mismatched materials enables an integration of electronic and photonic devices and provides a much wider range of design parameters like the band gaps or effective masses.<sup>2-4</sup> In the past 10 years, the optical and structural properties of the  $\text{In}_x\text{Ga}_{1-x}\text{As}/\text{GaAs}$  system have been widely studied because of potential applications in opto-electronic devices.<sup>1-4</sup>

Some previous work has focused on the investigation of misfit dislocations and the associated dark line defects (DLDs) with spatially resolved experiments like scanning cathodoluminescence (CL), transmission electron microscopy (TEM), and a combination of both methods.<sup>5-7</sup> While the temperature dependence of luminescence in quantum wells and superlattices has been investigated previously,<sup>8,9</sup> little work that addresses the effects of thermal quenching of luminescence by misfit dislocations has been reported. Thermal quenching of the luminescence intensity has been interpreted in several ways by different authors, and has been attributed to either thermal dissociation of excitons and thermally activated nonradiative recombination,<sup>10</sup> or due to thermal emission of carriers out of the QW, resulting in a reduction of luminescence intensity at higher temperatures.<sup>11</sup> This paper will demonstrate that misfit dislocations and point defects caused by relaxation of strain can influence the behavior of thermal quenching of luminescence in  $\text{In}_x\text{Ga}_{1-x}\text{As}/\text{GaAs}$  multiple quantum wells.

## EXPERIMENTAL PROCEDURE

The sample examined in the present study consists of 44 periods of 65 Å-thick  $\text{In}_{0.21}\text{Ga}_{0.79}\text{As}$  quantum well and 400 Å-thick GaAs barriers grown on (001) semi-insulating GaAs substrate by molecular beam epitaxy. Details of the growth procedure have been previously described for similar samples.<sup>5</sup> The sample was investigated with scanning CL microscopy.

Cathodoluminescence measurements were performed with a JEOL 840-A thermionic emission scanning electron microscope. The luminescence emitted from the sample was collected with an ellipsoidal mirror which focuses radiation onto a coherent optical fiber bundle. A North Coast liquid nitrogen cooled EO-817 Ge p-i-n detector was used to measure the signal dispersed by a 0.25 m monochromator. An electron beam current of about 7 nA and beam energy of 20 keV was used to probe the sample. CL spectra and images were recorded for various different temperatures between 86 and 250 K.

## RESULTS AND DISCUSSION

The temperature dependence of the CL intensity is shown in Fig. 1 for temperatures between 86 and 250 K in a semilogarithmic plot versus reciprocal of temperature. The data corresponds to the integrated CL spectral intensity,  $I_{MQW}$ , of the MQW excitonic transition measured while the electron beam was scanning a  $128 \times 94 \mu\text{m}^2$  region. This plot is labeled A in Fig. 1. The CL intensity is reduced by about 2 orders of magnitude as we increase the temperature from 86 to 250 K. From Fig. 1, it is evident that there exists two temperature ranges which show an Arrhenius behavior. This behavior indicates the presence of two different thermally activated processes responsible for the reduction in luminescence efficiency. The slope of the straight line portions of the curves gives the activation energies for the two cases. The intensity  $I_{MQW}$  decreases exponentially as a function of  $1/T$  between 86 and 150 K with a corresponding activation energy of  $\sim 27$  meV and with an activation energy of  $\sim 79$  meV for the high temperature range (150 to 250 K).

In order to study local variations in activation energy we performed CL imaging at various different temperatures between 86 and 250 K. The spectral resolution was maintained at  $\sim 10$  nm to obtain an integrated CL intensity image for all temperatures. A scanning area of  $128 \times 94 \mu\text{m}^2$  in this study is discretized into  $640 \times 480$  pixels. For every single spatial position  $(x,y)$ , the activation energy ( $E_a$ ) was determined and a gray-scale image representing the activation energies is generated. In order to determine  $E_a$  at each pixel position, 14 images were obtained for various fixed temperatures between 86 and 250 K. The slopes were determined separately for the two temperature ranges observed in Fig. 1 using a least-squares fitting at each  $(x,y)$  position.

The CL image obtained at 86 K is shown in Fig. 2(a). Figure 2(b) represents a spatial mapping of the activation energies for the same region shown in Fig. 2(a) for the intermediate temperature range (86-150 K). Figure 2(c) represents a spatial mapping of the activation energies obtained in the high temperature range (150-250 K). The mapping of  $E_a$  into a gray-scale representation is shown by the gray bar indicating the activation energy scale. Plots of  $I_{MQW}$  vs.  $1/T$  are shown in Fig. 1 for two arbitrary local regions, labeled B and D (for bright and dark regions). Long streaks of constant gray shade are seen to run along the high symmetry  $\langle 110 \rangle$  directions in Fig. 2(b). These streaks correlate with the position and orientation of dark line defects (DLDs) of this sample observed in Fig. 2(a). In monochromatic CL imaging, dislocations appear as dark line defects (DLDs) as a result of a localized reduction of luminescence efficiency

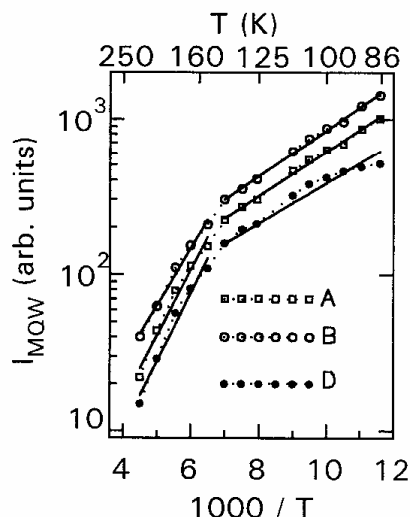


Fig. 1 Temperature dependence of CL intensity originating from the 65 Å MQW. The solid lines describe the exponential temperature dependence while the dotted lines connecting the data points are just used as a guide to the eye.

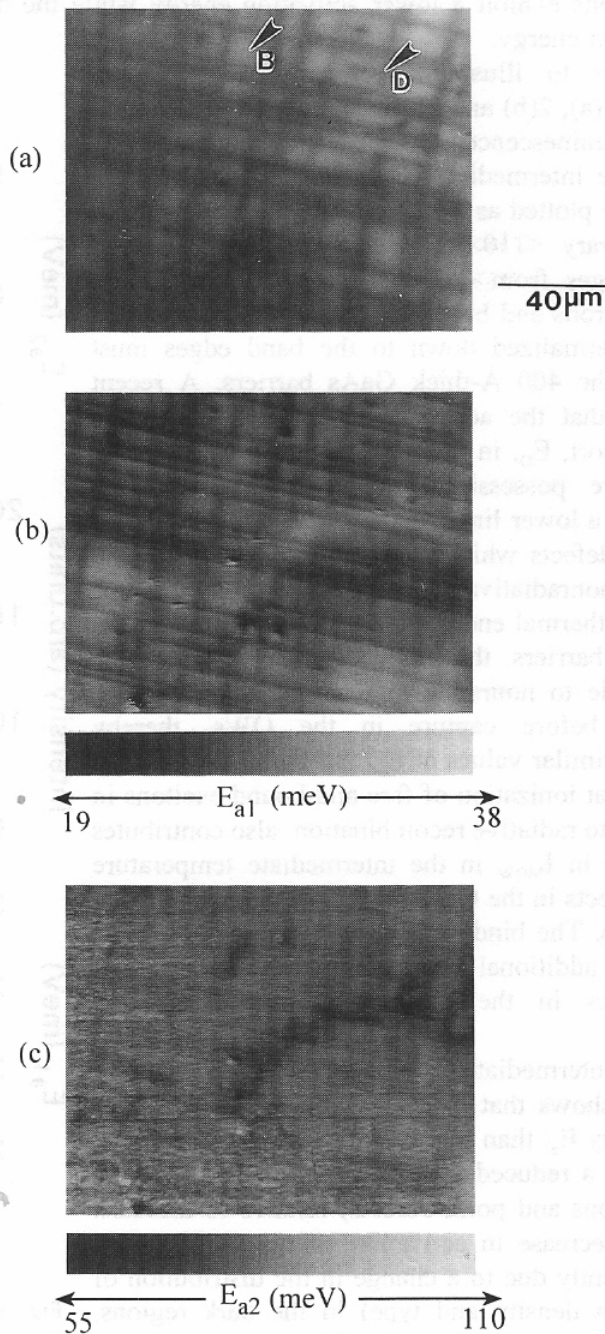


Fig. 2. The integrated CL intensity, and the mapping of the activation energies  $E_{a1}$  and  $E_{a2}$  in (a), (b), and (c), respectively. A scale showing the mapping of activation energies is shown in (b) and (c).

due to enhanced nonradiative recombination.<sup>5</sup> Comparing Figs. 2(a) and 2(b) we observe that regions containing misfit dislocations (dark regions) show a lower activation energy [gray regions in Fig. 2(b)] than regions which contain no defects [bright regions in Fig. 2(a)]. However, in the

high temperature range [Fig. 2(c)], there is a reversal of contrast as compared to Fig. 2(a), i.e. the bright regions exhibit a lower activation energy while the dark regions (DLDs) exhibit a higher activation energy.

In order to illustrate the correlation existing between Figs. 2(a), 2(b) and 2(c), a histogram is shown in Fig. 3. The luminescence intensity, and the activation energies for the intermediate ( $E_{a1}$ ) and high temperature regime ( $E_{a2}$ ) are plotted as a function of the distance taken along an arbitrary  $\langle 110 \rangle$ -oriented line. The activation energy  $E_{a1}$  ranges from  $\sim 23$  to 30 meV. Prior to the capture of electrons and holes into the QWs, free carriers which have thermalized down to the band edges must diffuse along the 400 Å-thick GaAs barriers. A recent study showed that the activation energy for ambipolar diffusive transport,  $E_D$ , in a nipi-doped  $\text{In}_{0.2}\text{Ga}_{0.8}\text{As}/\text{GaAs}$  MQW structure possessing similar barrier and QW thicknesses has a lower limit of  $\sim 29$  meV.<sup>12</sup> It is plausible that the same defects which impede ambipolar diffusion also serve as nonradiative recombination centers. Thus, once sufficient thermal energy is attained to surmount the defect-induced barriers, the mobile carriers also become more susceptible to nonradiative recombination at these same centers before capture in the QWs, thereby explaining the similar values of  $E_{a1}$  and  $E_D$ . Likewise, it is also possible that ionization of free and bound excitons in the QWs, prior to radiative recombination, also contributes to the decrease in  $I_{\text{MQW}}$  in the intermediate temperature range since defects in the QWs should also exhibit similar thermal barriers. The binding energy of the exciton is  $\sim 7$  meV, requiring additional thermal activation over defect-induced barriers in the QWs prior to nonradiative recombination.

For the intermediate temperature range (86-150 K), the histogram shows that bright regions exhibit a larger activation energy  $E_{a1}$  than that of dark regions. The bright regions contain a reduced defect density (i.e., density of misfit dislocations and point defects) relative to the dark regions. This decrease in activation energy for the dark regions is evidently due to a change in the distribution of defects (both in density and type) in the dark regions. Consistent with the above description, we expect that diffusing carriers in the GaAs barriers of dark regions will experience an enhanced probability for nonradiative recombination prior to their capture in the InGaAs QWs, in accordance with a reduction in  $E_{a1}$ .

The mismatch strain present at the interface between the InGaAs QWs and the GaAs barrier is relieved by the creation of misfit dislocations. The substrate possesses a fixed number of threading dislocation sources and substrate surface defects and impurities which act as

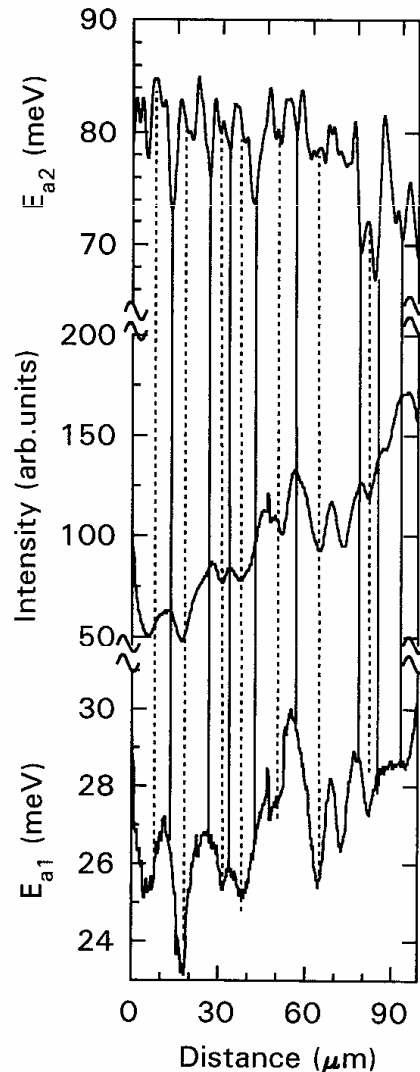


Fig. 3 Histogram of CL intensity, and activation energies ( $E_{a1}$  and  $E_{a2}$ ) for an arbitrary line scan done along the  $\langle 110 \rangle$  orientation.

heterogeneous nucleation sites for  $60^\circ$  threading dislocations. Once the thickness of the epilayer, during the  $\text{In}_x\text{Ga}_{1-x}\text{As}/\text{GaAs}$  MQW growth, has reached a value where the strain force is equal to the dislocation line tension which resist the elongation of the dislocation, the dislocation will glide laterally on a  $\{111\}$  slip plane, resulting in an interfacial misfit dislocation.<sup>13,14</sup> The general treatment of Matthews and coworkers has yielded an equilibrium model for determination of heteroepitaxial critical thicknesses.<sup>14</sup> Dislocation elongation is an activated process which is controlled by frictional forces such as the Peierls force.<sup>15</sup> Likewise, the presence of surface steps, Cottrell atmosphere of point defects and impurities can affect the kinetics of glide or climb of the dislocation. It has been observed that the presence of misfit dislocations results in a local reduction in compressive stress accompanied by a local decrease in band-gap.<sup>16</sup> This local reduction in stress near regions containing misfit dislocations would result in fluctuations of the band-gap along the interface. Theoretical calculations using the transfer-matrix method (TMM) were used to determine the energy states for both a fully strained and a fully relaxed MQW. The conduction to valence band offset ratio is taken as 70/30, and is assumed to be independent of  $x$ . Further, in order to accurately determine the potential profile, strain induced effects associated with the  $\text{In}_{0.21}\text{Ga}_{0.79}\text{As}/\text{GaAs}$  interface was also taken into account. A more detailed account of the method used for determining the potentials is presented elsewhere.<sup>17</sup>

	$E_{BC}$ (meV)	$E_{BV}$ (meV)
Fully Strained	111	58
Fully Relaxed	159	80

Table I.  $E_{BC} = \Delta E_C - E_{e1}$  and  $E_{BV} = \Delta E_V - E_{hh1}$ , are the effective barrier heights for re-emission out of the quantum well in the conduction and the valence band respectively, where  $\Delta E_C$  and  $\Delta E_V$  are the conduction and valence band offsets between  $\text{In}_{0.21}\text{Ga}_{0.79}\text{As}$  and GaAs, and  $E_{e1}$  and  $E_{hh1}$  denote the calculated first electron and heavy-hole subband energy.

The activation energy  $E_{a2}$  is most likely a result of re-emission of carriers which have been captured in the QWs since  $E_{a2}$  varies from  $\sim 65$  to  $\sim 85$  meV. A similar re-emission of captured carriers has previously been observed in AlGaAs/GaAs MQW systems.<sup>11</sup> Consider a region which contains misfit dislocations. The local reduction in strain in these regions results in lowering of the band-gap and an increase in the effective barrier height for electrons ( $E_{BC}$ ) and holes ( $E_{BV}$ ) as compared to the effective barrier height for electrons and holes for a bright region. It is possible that the enhanced activation energy exhibited by the dark regions in Fig. 2(a) is due to the larger barrier heights for carrier re-emission exhibited in the partially relaxed regions. The limiting cases for the QW barrier heights are illustrated in Table I, and these energies for the partially-relaxed regions will be intermediate to the fully strained and relaxed cases. In the high temperature range (150-250 K), the bright regions exhibit a lower activation energy which is consistent with the lower effective barrier height for electrons and holes listed in Table I in a quantum well subject to a larger strain. The DLDs [dark regions in Fig. 2(a)] correspond to regions of higher activation energy  $E_{a2}$ , as seen in the histogram of Fig. 3 and is consistent with a higher barrier height caused by the strain relaxation. Another explanation for the converse behavior of the  $E_{a1}$  and  $E_{a2}$  activation energies may relate to the density of defects in the GaAs barriers. The enhanced density of defects in the dark regions will impede thermally re-emitted carriers from drifting away from the QWs, thereby enhancing the probability of recapture into

the QWs. This enhanced defect density may increase effectively the barrier height for the phenomenon of thermal re-emission. From the present data, however, it is not possible to determine as to which of these two explanations for the change in  $E_{a2}$  near DLDs is the dominant effect.

## CONCLUSIONS

We have studied the temperature dependence of CL intensity from  $\text{In}_{0.21}\text{Ga}_{0.79}\text{As}/\text{GaAs}$  multiple quantum wells. We have observed local variations in the activation energy, which is likely caused by local fluctuations in the band edge near misfit dislocations and point defects. A pronounced decrease in CL intensity occurs for both the bright and the dark regions above 150 K. The magnitude of activation energies observed for the temperatures greater than 150 K indicates that this decrease is probably due to the thermal re-emission of electrons or holes from the quantum wells.

## ACKNOWLEDGEMENTS

This work was sponsored by the U.S. Army Research Office and the National Science Foundation.

## REFERENCES

1. J.J. Rosenberg, M. Benlamri, P.D. Kirchner, J.M. Woodall, and G.D. Petit, *IEEE Electron. Dev. Lett.* EDL-6, 491 (1985).
2. G.C. Osburne, *Phys. Rev. B* **27**, 5126 (1983).
3. G.E. Bir and G.L. Pikus, *Symmetry and Strain Induced Effects in semiconductors* (Wiley, New York, 1974).
4. J.E. Schirber, I.J. Fritz, and L.R. Dawson, *Appl. Phys. Lett.* **46**, 461 (1985).
5. D.H. Rich, T. George, W.T. Pike, J. Maserjian, F.J. Grunthaner, and A. Larsson, *J. Appl. Phys.* **72**, 5834 (1992).
6. E.A. Fitzgerald, G.D. Ast, P.D. Kirchner, G.D. Petit, and J.M. Woodall, *J. Appl. Phys.* **63**, 693 (1988).
7. K.L. Kavanagh, M.A. Capano, L.W. Hobbs, J.C. Barbour, P.M.J. Maree, W. Schaff, J.W. Mayer, G.D. Petit, J.A. Stroschio, and R.M. Feenstra, *J. Appl. Phys.* **68**, 2739 (1990).
8. D. Bimberg, J. Christen, A. Steckenborn, G. Weimann, and W. Schlapp, *J. Lumin.* **30**, 562 (1985).
9. K. Uno, K. Hirano, S. Noda, and A. Sakaki, *Proceedings of the 19th International Symposium on GaAs and Related Compounds* (IOP, Bristol, 1993), p. 241.
10. D.S. Jiang, H. Jung, and K. Ploog, *J. Appl. Phys.* **64**, 1371 (1988).
11. U. Jahn, J. Menninger, R. Hey, and H.T. Grahn, *Appl. Phys. Lett.* **64**, 2382 (1994).
12. D.H. Rich, K. Rammohan, Y. Tang, H.T. Lin, J. Maserjian, F.J. Grunthaner, A. Larsson, and S.I. Borenstain, *Appl. Phys. Lett.* **64**, 730 (1994).
13. C.A.B. Ball and J.H. Van der Merwe, *Dislocations in Solids*, (North-Holland, Amsterdam, 1983), Chap. 27.
14. J.W. Matthews and A.E. Blakeslee, *J. Cryst. Growth.* **27**, 118 (1974).
15. B.A. Fox and W.A. Jesser, *J. Appl. Phys.* **68**, 2801 (1990).
16. K. Rammohan, Y. Tang, D.H. Rich, R.S. Goldman, H.H. Wieder, and K.L. Kavanagh, *Phys. Rev. B* **51**, 5033 (1995).
17. D. H. Rich, H.T. Lin, and A. Larsson, *J. Appl. Phys.*, in press.